AD_____

GRANT NO: DAMD17-94-J-4080

TITLE: Topology and Function of Human P-glycoprotein in Multidrug
Resistant Breast Cancer Cells

PRINCIPAL INVESTIGATOR(S):   Ernest S. Han
                        Luis Reuss, M.D.

CONTRACTING ORGANIZATION: University of Texas Medical Branch
                        Galveston, Texas 77555-0136

REPORT DATE: September 1995

```
  _____
 | S DTIC          D |
 |   ELECTE          |
 |   DEC 0 8 1995    |
 |       G           |
 |_____|
```

TYPE OF REPORT: Annual

PREPARED FOR: Commander
                U.S. Army Medical Research and Materiel Command
                Fort Detrick, Maryland 21702-5012

DISTRIBUTION STATEMENT: Approved for public release;
                        distribution unlimited

                              DTIC QUALITY INSPECTED 3

19951204 085

REPORT DOCUMENTATION PAGE

Form Approved
OMB No. 0704-0188

Public reporting burden for this collection of information is estimated to average 1 hour per response, including the time for reviewing instructions, searching existing data sources, gathering and maintaining the data needed, and completing and reviewing the collection of information. Send comments regarding this burden estimate or any other aspect of this collection of information, including suggestions for reducing this burden, to Washington Headquarters Services, Directorate for Information Operations and Reports, 1215 Jefferson Davis Highway, Suite 1204, Arlington, VA 22202-4302, and to the Office of Management and Budget, Paperwork Reduction Project (0704-0188), Washington, DC 20503.

1. AGENCY USE ONLY (Leave Blank)	2. REPORT DATE September 1995	3. REPORT TYPE AND DATES COVERED Annual (9/1/94–8/31/95)

4. TITLE AND SUBTITLE
Topology and Function of Human P-glycoprotein in Multidrug Resistant Breast Cancer Cells

5. FUNDING NUMBERS
DAMD17-94-J-4080

6. AUTHOR(S)
Ernest S. Han
Luis Reuss, M.D.

7. PERFORMING ORGANIZATION NAME(S) AND ADDRESS(ES)
University of Texas Medical Branch
Galveston, Texas 77555-0136

8. PERFORMING ORGANIZATION REPORT NUMBER

9. SPONSORING/MONITORING AGENCY NAME(S) AND ADDRESS(ES)
U.S. Army Medical Research and Materiel Command
Fort Detrick, Maryland 21702-5012

10. SPONSORING/MONITORING AGENCY REPORT NUMBER

Accesion For
NTIS CRA&I	☒
DTIC TAB	☐
Unannounced	☐
Justification	

By
Distribution /

Availability Codes
| Dist | Avail and / or Special |
| A-1 | |

11. SUPPLEMENTARY NOTES

12a. DISTRIBUTION/AVAILABILITY STATEMENT
Approved for public release; distribution unlimited

12b. DISTRIBUTION CODE

13. ABSTRACT (Maximum 200 words)

Multidrug resistance is characterized by the overexpression of P-glycoprotein (Pgp), a 170-kDa glycoprotein coded by the MDR1 gene in humans. Pgp actively extrudes chemotherapeutic agents and is related to swelling-activated chloride currents (I_{cl}^s). The goal of this research is to understand the relationship between Pgp structure and function. Pgp topology was studied in an *in vitro* system that generated truncated peptides of human *MDR1* and hamster *pgp1* Pgp, inserted into microsomal membranes. We conclude that the C-terminal half topologies of hamster *pgp1* and human *MDR1* Pgp are different from the hydropathy-predicted model and from each other. Functional studies examined Pgp's role in I_{cl}^s. Using the whole-cell patch-clamp technique, we have shown that the addition of anti-Pgp monoclonal antibody (Mab) C219 to the pipette solution blocks I_{cl}^s in cells expressing Pgp (BC19/3 and KB-V1 cells). Other anti-Pgp Mabs and mouse IgG had no effect on I_{cl}^s. C219 had no effect on cells without Pgp expression (MCF-7 and BALB/c-3T3 cells). We conclude that Pgp has a regulatory role of I_{cl}^s, probably by specific association with swelling-activated Cl$^-$ channels.

14. SUBJECT TERMS
P-glycoprotein, channel, topology, multidrug resistance

15. NUMBER OF PAGES
19

16. PRICE CODE

17. SECURITY CLASSIFICATION OF REPORT	18. SECURITY CLASSIFICATION OF THIS PAGE	19. SECURITY CLASSIFICATION OF ABSTRACT	20. LIMITATION OF ABSTRACT
Unclassified	Unclassified	Unclassified	Unlimited

NSN 7540-01-280-5500

Standard Form 298 (Rev. 2-89)
Prescribed by ANSI Std. Z39-18
298-102

FOREWORD

Opinions, interpretations, conclusions and recommendations are those of the author and are not necessarily endorsed by the US Army.

_____ Where copyrighted material is quoted, permission has been obtained to use such material.

_____ Where material from documents designated for limited distribution is quoted, permission has been obtained to use the material.

_____ Citations of commercial organizations and trade names in this report do not constitute an official Department of Army endorsement or approval of the products or services of these organizations.

_____ In conducting research using animals, the investigator(s) adhered to the "Guide for the Care and Use of Laboratory Animals," prepared by the Committee on Care and Use of Laboratory Animals of the Institute of Laboratory Resources, National Research Council (NIH Publication No. 86-23, Revised 1985).

_____ For the protection of human subjects, the investigator(s) adhered to policies of applicable Federal Law 45 CFR 46.

X In conducting research utilizing recombinant DNA technology, the investigator(s) adhered to current guidelines promulgated by the National Institutes of Health.

X In the conduct of research utilizing recombinant DNA, the investigator(s) adhered to the NIH Guidelines for Research Involving Recombinant DNA Molecules.

X In the conduct of research involving hazardous organisms, the investigator(s) adhered to the CDC-NIH Guide for Biosafety in Microbiological and Biomedical Laboratories.
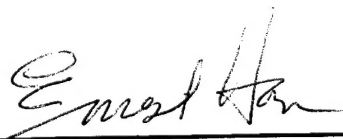
_____   9-20-95
PI - Signature   Date

TABLE OF CONTENTS

INTRODUCTION

Background and Significance

Treatment of breast and other cancers by chemotherapy has been often unsuccessful because cancer cells are intrinsically resistant or develop resistance to multiple chemotherapeutic agents (termed multidrug resistance or MDR) (1,2). MDR is characterized by the overexpression of P-glycoprotein (Pgp), a 170-kDa transmembrane glycoprotein coded by the MDR1 gene in humans. Pgp has been demonstrated to be an ATPase that actively extrudes various unrelated cytotoxic drugs out of cells. A question arises as to how Pgp can transport such a wide variety of substrates. Furthermore, it has been recently reported that Pgp may also be associated with volume-activated chloride channels (3,4). Since Pgp has such a diversity of functions, gaining insight to the structure of Pgp may offer insight into its functions. The goal of my research is to study the structure and function of Pgp in order to gain an understanding into the mechanism(s) of chemotherapy failure in breast cancer and other malignancies.

I. Structure of P-glycoprotein

Based on amino acid sequence analysis, P-glycoprotein belongs to the ATP-binding cassette (ABC) transporter superfamily, which includes the cystic fibrosis transmembrane conductance regulator (CFTR) (1,2). Hydropathy analysis of Pgp amino acid sequence predicts 2 homologous halves with each containing six transmembrane (TM) segments and a nucleotide-binding domain. However, alternate topologies for both the N- and C-terminal halves of Pgp have been reported (5-11).

Studies examining the N-terminal half of human MDR1, Chinese hamster pgp1, and mouse mdr1 Pgps have demonstrated a different topology for each Pgp species using a Xenopus Oocyte expression system (6,10), an in vitro translation system (7), and a bacterial expression system (9), respectively. However, a similar model was generated for the N-terminal half of Chinese hamster pgp1 and mouse mdr1 Pgps when an in vitro system was used to study both Pgp species (5,7). For the C-terminal half of Pgp, alternate membrane topologies have been reported only for human MDR1 (6) and mouse mdr1 (5,12) Pgps and not Chinese hamster pgp1 Pgp. For human MDR1 Pgp, Skach et al. (6) showed that TM8 and TM9 are not in the membrane (Fig. 1) using both a Xenopus oocyte expression system and in vitro translation system. In contrast, Béjà and Bibi (12) redefined the borders for TM7 and TM8 based on studies expressing the C-terminal half of mouse mdr1 Pgp in a bacterial system.

We hypothesize that the generation of a particular topology depends on the Pgp species and the system used to study the topology. For the period September 1,1994 - August 31, 1995, we focused our efforts on determining the topology of the C-terminal half of Chinese hamster pgp1 Pgp using an in vitro expression system. Furthermore, we compared human and hamster C-terminal half

Pgp topology using the same *in vitro* expression system.

II. Function of P-Glycoprotein

P-Glycoprotein has been suggested to be a bifunctional protein that can actively transport chemotherapeutic agents out of cells and may play a role in volume-activated chloride currents (4). The former has been well established (1,2), but the latter function is controversial. Valverde et al. (3) and Gill et al. (4) proposed a novel association between Pgp and swelling-activated Cl⁻ channels in two cell lines, NIH3T3 mouse fibroblasts and a lung epithelial cell line, transfected with human *MDR1* cDNA. However, other studies did not confirm these conclusions, showing a lack of correlation between Pgp expression and swelling-activated Cl⁻ currents (I_{Cl}') (12-18).

We have demonstrated that Pgp expression is associated with I_{Cl}' in human breast cancer cells transfected with the human *MDR1* cDNA (BC19/3 cells). This association was found when the cells were detached from the substratum. Interestingly, no difference in I_{Cl}' was found between drug-sensitive human breast cancer cells (MCF-7 cells) and multidrug-resistant BC19/3 cells when the cells were substratum-attached. Also studies have shown that the degree of cell swelling required for current activation may differ between wild-type and Pgp-expressing cells (14,16). These observations suggest a potential association between Pgp expression and I_{Cl}'. To ascertain the specificity of the relationship between Pgp and I_{Cl}', we tested the anti-Pgp monoclonal antibody C219 under the whole-cell patch clamp configuration.

BODY OF ANNUAL REPORT

METHODS

I. <u>Membrane topology of human *MDR1* Pgp and Chinese hamster *pgp1* Pgp in microsomal membranes</u>

I.1 *cDNA constructs and in vitro transcription*

cDNA fragments encoding the 6 putative transmembrane segments of the C-terminal half of human *MDR1* and hamster *pgp1* Pgp were subcloned into pGEM-4z expression vector to generate pGHuPGP-C6 and pGHaPGP-C6, respectively. Additional potential N-linked glycosylation sites in pGHuPGP-C6 (amino acids 839 and 842) and pGHaPGP-C6 (amino acids 836 and 839) were generated by site-directed mutagenesis PCR technique. The wild type and mutant cDNA template were then linearized with different restriction enzymes and transcribed with SP6 polymerase in the presence of a cap analog $m^7G(5')ppp(5')G$. Following transcription, we removed the DNA template with RQ1 DNase and purified the RNA transcripts.

I.2 *Translation using a cell-free system*

Translation of RNA transcripts was performed using the rabbit reticulocyte translation system in the absence or presence of dog pancreatic microsomal membranes (RM) as suggested by the supplier (Promega). Membrane (pellet) and soluble (supernatant) fractions were separated by centrifugation at 4°C. To determine whether the translated peptides were integrally-associated with the membrane, the RM fraction was treated with Na_2CO_3 (pH 11.7) to remove content and peripherally-associated peptides. Experiments involving protease digestion of membrane fractions was performed by incubation of RM with proteinase K. The reaction was stopped by addition of 10 mM phenylmethylsulfonyl fluoride (PMSF). The membrane fraction was then microfuged and washed in STBS (in mM: 250 sucrose, 10 Tris-HCl, pH 7.5, 150 NaCl) containing PMSF. For endoglycosidase treatment with PNGase F, samples were microfuged and the pellet resuspended in a reaction buffer containing 50 mM phosphate buffer (pH 7.6), 1.25% Nonidet P-40, 0.5% 2 mercaptoethanol, 2 mM PMSF, 1 unit PNGase F, and 0.2% SDS. The reaction was incubated for 1 hr at 37°C and stopped by the addition of electrophoresis sample buffer. For immunoprecipitation reactions, samples were incubated with anti-Pgp polyclonal antibody α-Pgp-L8 overnight at 4°C and then incubated with Protein A beads for at least 2 hrs at room temperature. Following centrifugation, the pellet was washed twice in a buffer containing 0.1% Triton X-100, 0.02% SDS, 150 mM NaCl, 50 mM Tris-HCl, pH 7.4, 5 mM EDTA, and 10 mM PMSF. All samples were analyzed by SDS-PAGE and fluorography.

II. <u>Functional analysis of human *MDR1* Pgp by whole-cell patch clamp technique</u>

II.1 *Cells*

Four different cell types were used in this report: (1) MCF-7 cells, human breast cancer cell line, (2) BC19/3 cells, MCF-7 cells transfected with the human MDR1 cDNA, (3) BALB/c-3T3 cells, mouse fibroblast cell line, and (4) KB-V1 cells, a multidrug-resistant HeLa cell line. Cells were plated on coverslips 1 day prior to the experiment in the absence of chemotherapeutic agents.

II.2 *Electrophysiology*

To achieve whole-cell patch-clamp configuration, pipettes with resistances of 4-7 MΩ were used to obtain gigaohm seals, which were ruptured by additional negative pressure. Steady-state currents were measured at various voltages (-80 to +80 in 20 mV steps), 40 ms after the start of the voltage pulse. Bath and pipette solution composition were as follows (in mM): NMDG-Cl pipette (280 mosmol/kg)- 140 N-methyl-D-glucamine chloride (NMDGCL), 1.2 $MgCl_2$, 1 EGTA, 10 HEPES, 2 ATP, 0.5 GTP; Bath isosmotic (280 mosmol/kg)- 140 NMDGCL, 1.3 $CaCl_2$, 0.5 $MgCl_2$, 10 HEPES, 8 glucose; Bath hyposmotic (220 mosmol/kg)- 105 NMDGCL, 1.3 $CaCl_2$, 0.5 $MgCl_2$, 10 HEPES, 8 glucose; All solutions were titrated to pH 7.4 and filtered.

II.3 *Unidirectional efflux of Rhodamine 123*

Cells were loaded with 1 or 10 μM rhodamine 123 (R123) in a HEPES-buffered solution (HBS) at room temperature for 1 hr and then mounted on a fluorescence microscope. Cells were superfused with HBS without R123 and a decay in the fluorescence signal was measured. The efflux rate constant (k) was determined from the best simple-exponential fit to the data.

II.4 *Immunofluorescence*

Cells were fixed and permeabilized in cold acetone at -20°C followed by air drying. After incubation in a blocking solution (1:10 mouse serum in PBS/BSA solution), cells were incubated with 1 μg/ml FITC-labeled C219 for 2 hrs at room temperature. After washing in PBS solution, cells were visualized by confocal microscopy.

II.5 *Western blot analysis*

Western blots were done with membranes prepared by differential centrifugation, as previously described (ref.*). Membrane proteins were subjected to SDS-PAGE and transferred to a PVDF membrane. The membranes were blocked with 10% non-fat dry milk in Tris-buffered saline (TBS) and incubated with 1 μg/ml of one of the following anti-Pgp monoclonal antibodies (Mabs): C219, C494, or JSB-1. Incubation for 2 hrs in TBS containing 1% non-fat dry milk and 0.1% Tween 20. The secondary antibody was a horseradish

peroxidase-sheep anti-mouse IgG (1/2500 dilution for 1 hr). After incubation with each antibody, membranes were subjected to three 10-min washes with TBS. Detection was by enhanced chemiluminescence. Membranes were stripped following the protocol from Amersham. Before reprobing, the membranes were analyzed by ECL using secondary antibody alone.

RESULTS

I.   <u>Topological analysis of Pgp</u>

I.1 *The C-terminal half of Chinese hamster pgp1 Pgp is glycosylated in microsomal membranes*

A cDNA construct encoding the 6 putative transmembrane segments (TMs) of the C-terminal half of hamster *pgp1* Pgp (pGHaPGP-C6) was used to synthesize RNA transcripts *in vitro* (Fig. 1). We then used the rabbit reticulocyte lysate (RRL) translation system supplemented with dog pancreatic microsomes (RM) to generate peptides from the *in vitro* synthesized RNA transcripts.
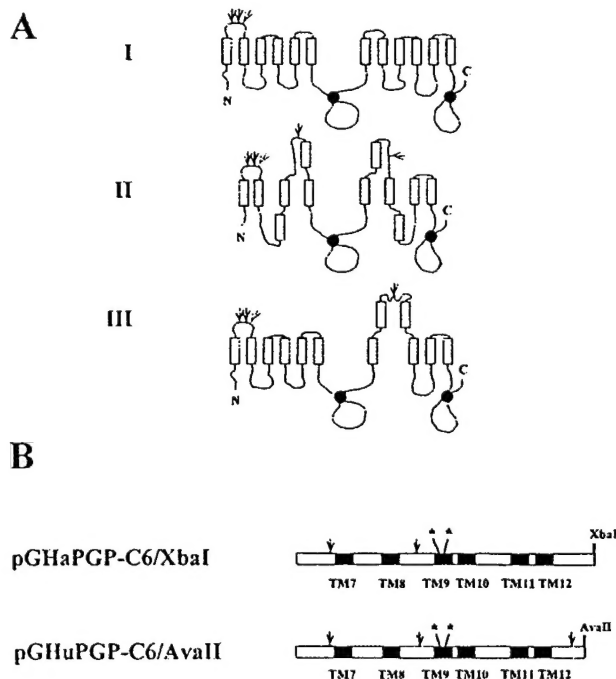

Figure 1. A. Topological models of Pgp. Model I was proposed from previous studies on hydropathy analysis of Pgp protein sequence (19) Model II was based on studies from mouse *mdr1* Pgp (5) and this current report on hamster pgp1 Pgp. Model III represents human *MDR1* Pgp as proposed by Skach et al. (6). B. Schematic diagram of RNA transcripts derived from C-terminal half hamster *pgp1* Pgp (pGHaPHP-C6) and human *MDR1* Pgp cDNA construct (pGHuPGP-C6). Transcripts were named according to the template cDNA construct followed by the restriction enzyme used to linearize the cDNA. Putative transmembrane segments are represented by solid bars, and nonhydrophobic sequences are shown as open bars. Potential glycosylation sequences are represented by branched symbols, where as the asterisk represents point mutations in which new potential glycosylation sites were generated.

9

The pGHaPGP-C6/XbaI transcript encodes the 6 TM segments of the C-terminal half hamster *pgp1* Pgp with a predicted molecular mass of 53 kDa. In the absence of RM, translation of pGHaPGP-C6/XbaI transcript resulted in a 48-kDa protein product (Fig. 2). The discrepancy in molecular weight between predicted and experimental results was due to anomalous mobility on SDS-PAGE and not due to premature termination or internal initiation of translation (data not shown). However in the presence of RM, 48- and 53-kDa bands were generated (Fig. 2).
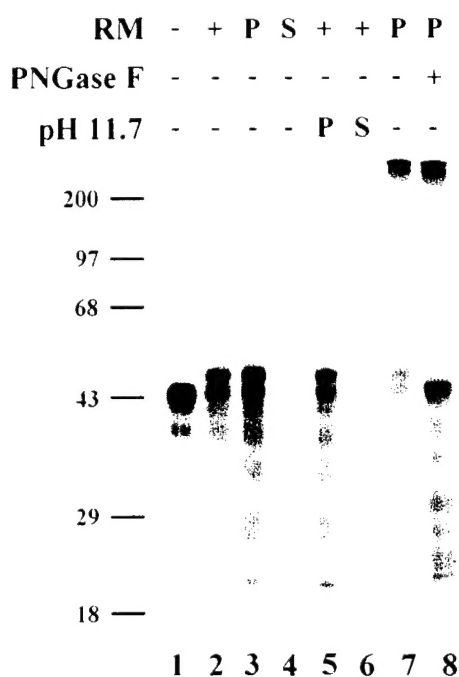
Figure 2. Glycosylation of the C-terminal half of hamster *pgp1* Pgp in microsomal membranes. Translation of pGHaPGP-C6/XbaI using rabbit reticulocyte lysate translation system in the absence (lane 1) or presence (lane 2) of dog pancreatic microsomal membrane (RM). The 53-kDa band in the presence of RM represents N-linked glycosylation of the 48-kDa product as confirmed by treatment of RM with the endoglycosidase, PNGase F (lanes 7 and 8). The 48- and 53-kDa products were associated with the membrane fraction after centrifugation (lanes 3 and 4) and integrally-associated with RM as demonstrated by Na_2CO_3, pH 11.7 treatment (lanes 5 and 6). P and S denote pellet and supernatant fractions, respectively.

Treatment with PNGase F, an endoglycosidase which removes N-linked oligosaccharides, shifted the 53-kDa protein product to 48 kDa (Fig. 2), indicating that the 53-kDa peptide was the glycosylated form of the 48-kDa peptide.

To further characterize the interaction of the nascent peptides with the microsomal membrane, we did several experiments. First, centrifugation separated the translation products into a membrane (pellet) and nonmembrane (supernatant) fraction. Both the 48- and 53-kDa peptides associated with the membrane fraction (Fig. 2). Treatment of the membrane fraction with Na_2CO_3 (pH 11.7), which

10

releases content and peripheral proteins from RM vesicles (20), demonstrated that both proteins were integrally-associated with the microsomal membranes (Fig. 2). These results demonstrate that the C-terminal half of hamster *pgp1* Pgp is a glycosylated, integrally-associated membrane protein. This implies that an alternate topology for the C-terminal half must exist because the hydropathy-generated model does not predict a glycosylated protein product (see Fig. 1).

I.2 *Glycosylation of the C-terminal half of hamster pgp1 Pgp is at the loop linking predicted TM8 and TM9.*

Based on studies by Zhang and Ling (5) on mouse *mdr1* Pgp and by Skach et al. (6) on human *MDR1* Pgp, we predicted that the most likely site of N-linked glycosylation occurred at the loop linking predicted TM8 and TM9. We tested this hypothesis by translating pGHaPGP-C6/*Xba*I transcript in the presence of RM and then exposing the microsomal membranes to proteinase K or proteinase K followed by PNGase F treatment. We would predict the presence of a ≈15-kDa protease-protected peptide that represents the amino acids from TM7 to TM9 of Pgp. Fig. 3 shows 14- and 17-kDa bands that are protected from protease digestion.
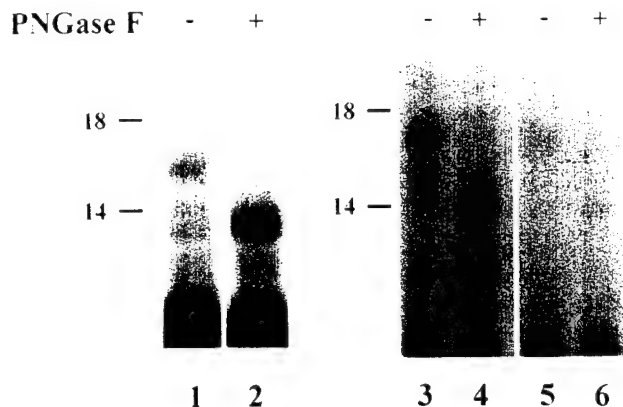

Figure 3. Glycosylation of the loop linking putative TM8 and TM9 in C-terminal half of hamster *pgp1* Pgp. Proteinase K digestion of RM (lane 1) resulted in the presence of 14- and 17-kDa bands. The 17-kDa protein product represented a glycosylated form of the 14-kDa product as demonstrated by a shift in molecular weight after PNGase F treatment (lane 1 vs. 2). These protease-protected bands could also be immunoprecipitated by a polyclonal antibody (α-Pgp-L8) generated against a peptide corresponding to the loop linking putative TM8 and TM9 (lanes 3 and 4), but not by preimmune serum (lanes 5 and 6).

Proteinase K digestion in the presence of 1% Triton X-100, which permeabilizes RM, resulted in no protected bands (data not shown). Exposure of the protease-protected peptides to PNGase F shifted the 17-kDa band to 14 kDa (Fig. 3), suggesting that the 17-kDa band was

glycosylated. Both the 14-kDa band and the glycosylated 17-kDa band represent the amino acids from TM7 to TM9, because both bands could be immunoprecipitated with a polyclonal antibody (α-Pgp-L8) generated against the loop between TM8 and TM9 of hamster *pgp1* Pgp (Fig. 3). The results imply that TM8 is not in the membrane as predicted and that the loop between TM7 and TM8 and the loop connecting TM8 and TM9 are extracellular in orientation.

I.3 *Hamster pgp1 Pgp and human MDR1 Pgp have different alternate topologies in microsomal membranes*

Various topological models have been postulated for Pgp. These variations may be due to different protein expression systems that were used to study the topology or the particular species of Pgp used. We wanted to determine whether the sequence differences between species confers a particular topology. The C-terminal half of hamster *pgp1* and human *MDR1* Pgp were directly compared using the rabbit reticulocyte lysate translation system in the presence of dog pancreatic microsomal membranes. Assuming that hamster and human Pgp had similar topologies, proteinase K digestion of RM was predicted to generate protease-protected peptides of similar molecular weight for both hamster and human species. Protease digestion of RM with hamster C-terminal half Pgp resulted in 14- and 17-kDa bands as noted previously. However, 20- and 23-kDa protein products were generated after protease digestion of RM with C-terminal half of human Pgp (Fig. 4).
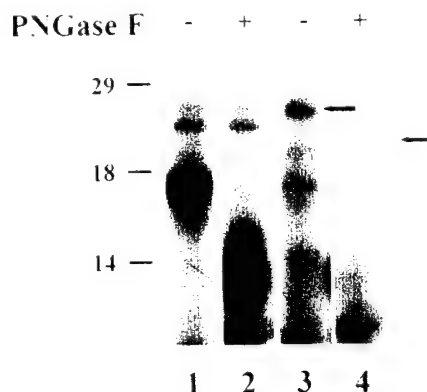

Figure 4. C-terminal half topology of hamster *pgp1* Pgp is different from human *MDR1* Pgp. Proteinase K digestion of hamster C-terminal half Pgp resulted in 14- and 17-kDa bands (lanes 1 and 2). The estimated size of the 14-kDa band correlated well with the calculated molecular weight of a peptide consisting of the amino acids from putative TM7 to TM9. In contrast 20- and 23-kDa protein products (lanes 3 and 4) were generated after protease digestion of human C-terminal half Pgp. The 20-kDa band corresponds closely to the calculated molecular weight of a peptide derived from amino acids from putative TM7 to TM10.

The 20-kDa band corresponded to the calculated molecular weight of a peptide derived from amino acids from putative TM7 to TM10. This

12

result suggests that hamster and human C-terminal half topology are different from each other when expressed in the rabbit reticulocyte lysate translation system.

II. Functional analysis of Pgp

II.1 *Plasma-membrane expression and transport function of Pgp in human breast cancer and other cell lines.*

We did the following experiments to assess Pgp expression in several cell types: immunoblots of membrane preparations, immunofluorescence studies and Rhodamine 123 (R123) efflux experiments. Western blot analysis in human breast cancer cells showed an immunoreactive band of ≈170 kDa with Mab C219 in BC19/3, but not in MCF-7 cells (Fig. 5). Similar results were obtained with two other anti-Pgp antibodies, C494 and JSB-1. Western blots of membranes of KB-V1 cells with C219 showed Pgp expression, while membranes of BALB/c-3T3 cells did not. For immunofluorescence studies, BC19/3 cells showed surface immunoreactivity, whereas MCF-7 cells were negative (Fig. 5).
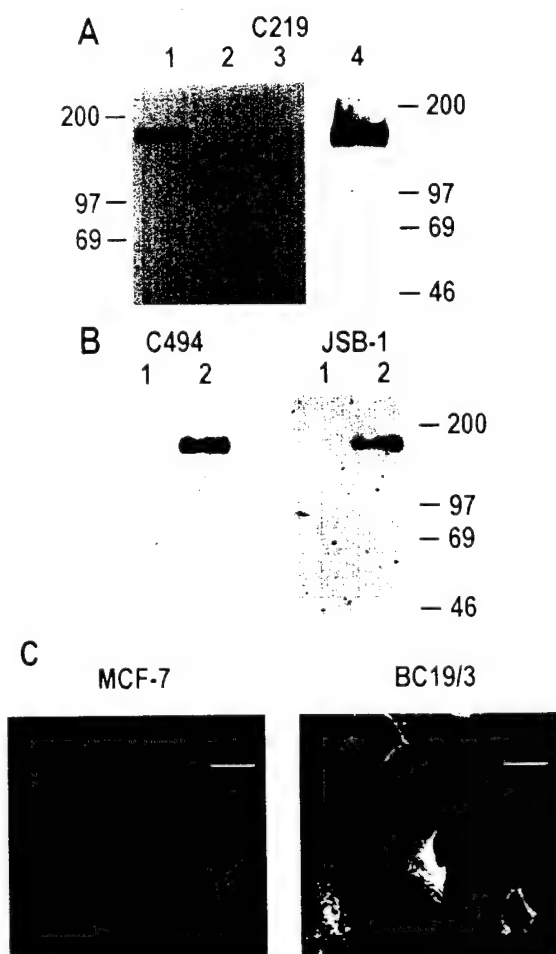

Figure 5. Western blot analysis and immunofluorescence studies. A. Western blot analysis of cell membrane proteins of BC19/3 (lane 1, 25 μg), MCF-7 (lane 2, 200 μg), BALB/c-3T3 (lane 3, 200 μg), and KB-V1 cells (lane 4, 10 μg) with C219 antibody. B. Western blot analysis of cell-membrane proteins of MCF-7 (lane 1, 100 μg) and BC19/3 cells (lane 2, 100 μg) with C494 or JSB-1 antibodies. A western blot was first carried out with C494, the membrane was then stripped and reprobed with JSB-1. C. Immunofluorescence studies of Pgp expression with FITC-labeled C219 in MCF-7 and BC19/3 cells. Bars denote 10 μm.

13

To test for functional expression of Pgp in these cell lines, we determined the unidirectional efflux of R123. Fig. 6B summarizes the efflux rate constants. Sizeable R123 efflux rate constants were found only in BC19/3 and KB-V1 cells.
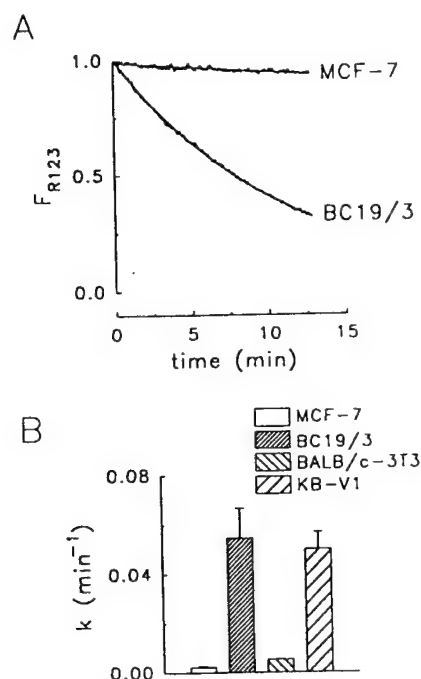
A

B

Figure 6. Unidirectional efflux of rhodamine 123 (R123). A. Typical time courses of decay in intracellular R123 fluorescence in MCF-7 and BC19/3 cells, loaded 1 h with 1 and 10 μM R123, respectively. Single-exponential fits are superimposed on the data. B. R123-efflux rate constants in MCF-7, BC19/3, BALB/c-3T3 and KB-V1 cells, calculated from single exponential fits.

II.2 *Mab C219 prevents I_{Cl}^s only in Pgp-expressing cells.*

To examine the possible association between Pgp and I_{Cl}^s, we tested the anti-Pgp Mab C219 under whole-cell patch clamp conditions. C219 has a cytoplasmic epitope on Pgp. Addition of 10 or 50 μg/ml C219 (final concentration) to the pipette solution virtually blocked I_{Cl}^s in BC19/3 cells and had no effect on MCF-7 cells (Fig. 7A). This result suggests a specific relationship between Pgp and I_s^{Cl}. To strengthen this conclusion, we tested (1) the effects of other immunoglobulins on I_{Cl}^s in BC19/3 cells and (2) the effects of C219 on I_{Cl}^s in other cells, with or without Pgp expression.

Fig. 7B shows the other immunoglobulins tested. F_{ab} fragments of C219 had similar effects as the whole C219 molecule. This rules out the possibility that the C219 effect is mediated by the F_c portion of the immunoglobulin. When a peptide analog of the C219 epitope (P15) was added in 100-fold molar excess along with C219, the C219 effect was abolished. P15 alone had no effect on I_{Cl}^s (data not shown). The addition of mouse IgG or other anti-Pgp antibodies with cytoplasmic epitopes (C494 or JSB-1) also had no effect on I_{Cl}^s.

14

These results show that the effect of C219 is not a result of nonspecific interactions of immunoglobulins within the cell.
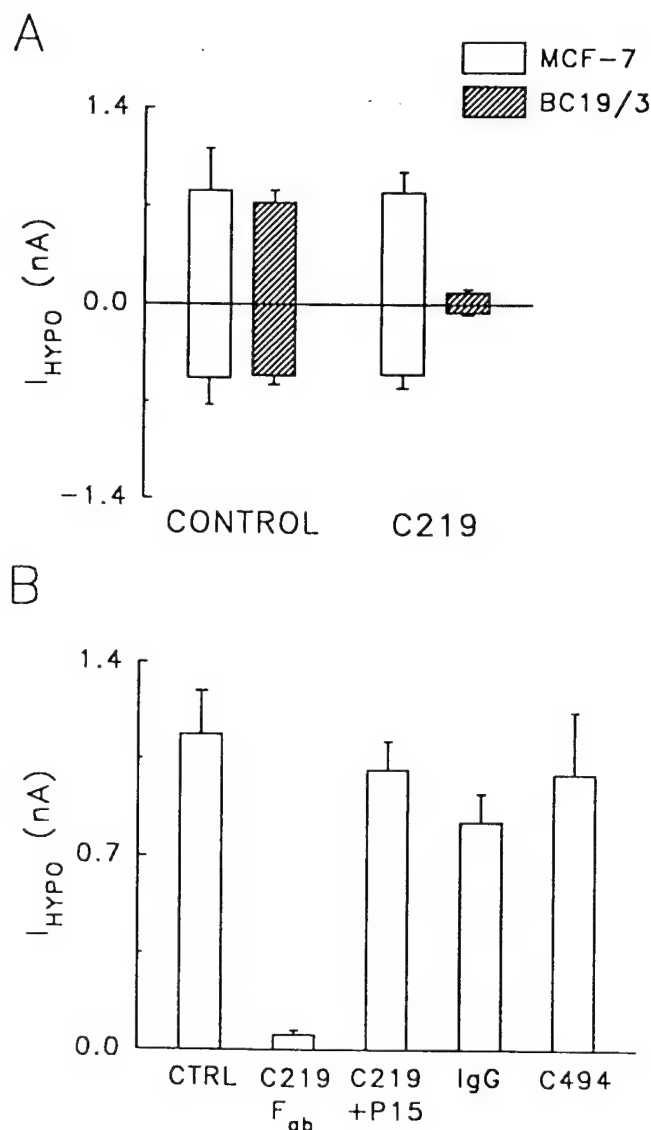
A

Figure 7. A. Effect of Mab C219 on I_{Cl}^s in BC19/3 cells. Data shown are I_{Cl}^s values at Vm -80 and 80 mV, pipette solution: NMDG-Cl, bath solution: NMDG-Cl (HYPO). Control (no Mab): MCF-7, n=5; BC19/3, n=7; C219 (10 or 50 μg/ml added to pipette solution): MCF-7 and BC19/3 cells, n=5. The difference between control and C219 in BC19/3 cells was statistically significant. B. Effects of antibodies on I_{Cl}^s in BC19/3 cells. I_{Cl}^s was measured at Vm = 80 mV, in hyposmotic NMDG-Cl solution, under control conditions (n=14) and in the conditions defined under the bars (C219 Fab fragments, C219 plus P15, mouse IgG, or C494 added to pipette solution; number of experiments: 3, 6, 4, and 3, respectively). Currents in the presence of C219 Fab fragments were significantly different from control (P < 0.05 vs. control experiments carried out the same days); other results were not significantly different from the respective controls.

B

Mab C219 was also tested in other cells that display I_{Cl}^s, with or without Pgp expression. Fig. 8 shows the I_{Cl}^s of BALB/c-3T3 and KB-V1 cells and the effect of C219. Challenge by hyposmotic bath solution generated similar current characteristics in the two cells, and differed from those in MCF-7 and BC19/3 cells in that

15

there was virtually no inactivation at positive membrane voltages. However, addition of the Mab C219 to the pipette solution had no effect on I_{Cl}^s in BALB/c-3T3 cells, but prevented activation in KB-V1 cells. These results indicate that the C219 effect occurs in cells expressing Pgp in the plasma membrane.
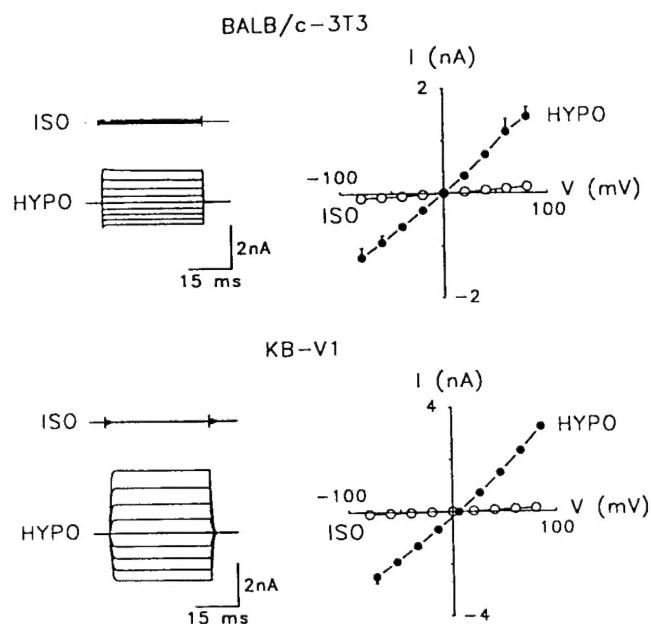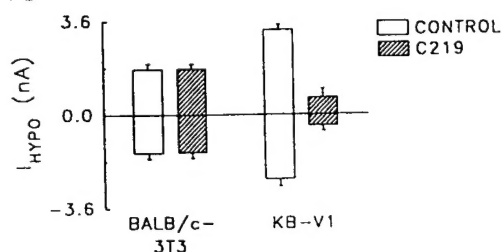

Figure 8. Effects of C219 on I_{Cl}^s in BALB/c-3T3 and KB-V1 cells. A. Whole-cell currents and current-voltage relationship in BALB/c-3T3 and KB-V1 cells. B. Effects of C219 on I_{Cl}^s were measured at Vm = 80 mV (positive bars) and at Vm = -80 mV (negative bars). BALB/c-3T3 cells: control, n = 5; C219, n = 4. KB-V1 cells: control and C219, n = 3. C219 (10 μg/ml) reduced I_{Cl}^s significantly in KB-V1 cells, but had no effect on I_{Cl}^s in BALB/c-3T3 cells.

CONCLUSIONS

This report shows that the C-terminal half of hamster *pgp1* Pgp has a topology different from the hydropathy-predicted model. Interestingly, this topology also differs from human *MDR1* Pgp topology. The difference between human and hamster C-terminal half Pgp topology was not due to using different expression systems. Instead, the different topologies resulted most likely from differences in the amino acid composition between human and hamster Pgp. It would be interesting to pursue the exact determinants that regulate Pgp topology. This information would be valuable in terms of "locking" Pgp into a particular topology and allowing functional analysis of the identified topology (as proposed in Task 2 in Statement of Work).

The effect of C219 on swelling-activated chloride currents in Pgp-expressing cells has provided evidence for a specific association between Pgp and swelling-activated chloride currents. However, this conclusion does not prove that Pgp is (a) a chloride channel itself or (b) a regulator of endogenous chloride channels. With the result of the C219 effect, one can assess the ion transport function of Pgp with C219 by the whole-cell patch clamp technique as proposed in task 2 in Statement of Work. For example, once single conformations of Pgp can be generated, the ion transport function of Pgp can be analyzed from the effect of C219. Furthermore, the ability of C219 to affect ion transport function suggests the possibility of using other site-specific antibodies (generated to a particular region of Pgp) to understand Pgp structure/function. For example we showed in this report that an alternate topology may exist in which the loop between TM8 and TM9 was shown to be extracellular. An antibody generated against the loop between TM8 and TM9 (see Fig. 1) could be tested for effects on ion transport function when added to the extracellular solution (assuming the alternate topology existed).

REFERENCES

1. Roninson, I.B. Structure and function of P-glycoproteins. In: *Molecular and Cellular Biology of Multidrug Resistance in Tumor Cells*. Roninson, I.B., ed., Plenum Press, New York, pp. 189-213, 1991.

2. Gottesman, M.M. and Pastan, I. Biochemistry of multidrug resistance mediated by the multidrug transporter. *Ann. Rev. Biochem.*, 62: 385-427, 1993.

3. Valverde, M.A., Diaz, M., Sepúlveda, F.V., Gill, D.R., Hyde, S.C., and Higgins, C.F. Volume-regulated chloride channels associated with the human multidrug-resistance P-glycoprotein. *Nature* 355: 830-833, 1992.

4. Gill, D.R., Hyde, S.C., Higgins, C.F., Valverde, M.A., Mintenig, G.M., and Sepúlveda, F.V. Separation of drug transport and chloride channel functions of the human multidrug resistance P-glycoprotein. *Cell* 71: 23-32, 1992.

5. Zhang, J.-T. and Ling, V. Study of membrane orientation and glycosylated extracellular loops of mouse P-glycoprotein by in vitro translation. *J. Biol. Chem.*, 266:18224-18232, 1991.

6. Skach, W.R, Calayag, M.C. and Lingappa, V.R. Evidence for an alternate model of human P-glycoprotein structure and biogenesis. *J. Biol. Chem.*, 268:6903-6908, 1993.

7. Zhang, J.T., Duthie, M. and Ling, V. Membrane topology of the N-terminal half of the hamster P-glycoprotein molecule. *J. Biol. Chem.*, 268:15101-15110, 1993.

8. Zhang, J.T. and Ling, V. Membrane orientation of transmembrane segments 11 and 12 of MDR- and non-MDR-associated P-glycoproteins. *Biochim. Biophys. Acta* 1153: 191-202, 1993.

9. Bibi, E. and Béjà, O. Membrane topology of multidrug resistance protein expressed in Escherichia coli. *J. Biol. Chem.* 269: 19910-19915, 1994.

10. Skach, W.R. and Lingappa, V.R. Transmembrane orientation and topogenesis of the third and fourth membrane-spanning regions of human P-glycoprotein (MDR1). *Cancer Res.* 54: 3202-3209, 1994.

11. Béjà, O. and Bibi, E. Multidrug resistance protein (MDR)-alkaline phosphatase hybrids in Escherichia coli suggest a major revision in the topology of the C-terminal half of Mdr. *J. Biol. Chem.* 270: 12351-12354, 1995.

12. Altenberg, G.A., Vanoye, C.G., Han, E.S., Deitmer, J.W. and Reuss, L. Relationship between rhodamine 123 transport, cell volume, and ion-channel function of P-glycoprotein. *J. Biol. Chem.*, 269: 7145-7149, 1994.

13. Dong, Y., Chen, G., Duran, G.E., Kouryama, K., Chao, A.C., Sikie, B.I., Gollapudi, S.V., Gupta, S., and Gardner, P. Volume-activated chloride current is not related to P-glycoprotein overexpression. *Cancer Res.* 54: 5029-5032, 1994.

14. Ehring, G.R., Osipchuk, Y.V., and Cahalan, M.D. Swelling-activated chloride channels in multidrug-sensitive and -resistant cells. *J.Gen. Physiol.* 104: 1129-1161, 1994.

15. Kunzelmann, K.I., Slotki, I.N., Klein, P., Koslowsky, T.,

Ausiello, D.A., Greger, R., and Cabantchik, Z.I. Effects of P-glycoprotein expression on cyclic AMP and volume-activated ion fluxes and conductances in HT-29 colon adenocarcinoma cells. *J. Cell. Physiol*. 161: 393-406, 1994.

16. Luckie, D.B., Krouse, M.E., Harper, K.L., Law, T.C., and Wine, J.J. Selection for MDR1/P-glycoprotein enhances swelling-activated K^+ and Cl^- currrents in NIH/3T3 cells. *Am. J. Physiol*. 267: C650-C658, 1994.

17. McEwan, G.T.A., Hirst, B.H., and Simmons, N.L. Carbachol stimulates Cl^- secretion via activation of two distinct apical Cl^- pathways in cultured human T84 intestinal epithelial monolayers. *Biochim. Biophys. Acta* 1220: 241-247, 1994.

18. Rasola, A., Galietta, L.J.V., Gruenert, D.C., and Romeo, G. Volume-sensitive chloride currents in four epithelial cell lines are not directly correlated to the expression of the MDR-1 gene. *J. Biol. Chem*. 269: 1432-1436, 1994.

19. Gottesman, M.M. and Pastan, I. The multidrug transporter, a double-edged sword. *J. Biol. Chem*. 263: 12163- 12166, 1988.

20. Howell, K.E. and Palade, G.E. Hepatic golgi fractions resolved into membrane and content subfraction. *J. Cell Biol*. 92: 822-832, 1982.